5. Pulsed Cathodic Vacuum Arc

5.1. Introduction

Continuous operation (DC) cathodic vacuum arcs (CVA) have been studied extensively within the School of Physics at the University of Sydney. Pulsed CVA's generally have a higher current and plasma density and also provide a more stable and reproducible plasma density than their DC counterparts. If a high repetition frequency can be achieved the deposition rate of pulsed CVA's is equal to or greater than that of DC arcs with a concomitant reduction in the rate of macroparticle formation. The development of the pulsed arc system described here was undertaken with the purpose of producing ultra-thin films and multilayers with finely controlled thickness, and for studying the sheath dynamics during PIII.

As shall be shown in chapters 7 and 8, when producing ultra-thin (<10nm) metallic and ceramic films, precise control over the deposition parameters is required. Filtered DC arcs exhibit density fluctuations on a millisecond timescale due to arc spot instabilities, and also on a timescale of a few seconds due to variations in the degree of plasma coupling to the magnetic macroparticle filter. Reproducible production of ultra-thin films is extremely difficult under these conditions. In contrast, a pulsed vacuum arc can provide a highly reproducible plasma density during each pulse. This allows the plasma density to be accurately controlled and facilitates the study of sheath dynamics during

PIII. Comparison with theoretical predictions can then be undertaken, as will be demonstrated in chapter 6. Films with pre-determined thicknesses can be deposited by measuring the amount of material deposited per pulse, and simply counting the number of pulses to achieve the required thickness.

A further motivation for the construction of a pulsed plasma source is the ability to produce plating-free implantation when combined with PIII. If a DC bias is applied to a substrate immersed in a pulsed arc plasma, the majority of ions within the plasma sheath will be implanted at the bias voltage. If the plasma is fully ionised, as is the case with a filtered cathodic vacuum arc, there is no deposition of neutral metal atoms during the pulse, resulting in pure MePIII. This method is converse to the more common method of pulse biasing the substrate in a DC arc plasma, which results in combined film deposition and implantation (MePIIID). Sroda *et al.* first demonstrated the concept with implantation of aluminium into silicon wafers [1]. Brown, Monteiro and Bilek developed a theoretical model for the sheath behaviour in a drifting plasma [2]. The results suggest that as long as the arc pulse remains short, the density is not too low, and the drift velocity of the plasma is high, then the sheath will not expand to the chamber walls during the pulse. Unfortunately, with high bias voltages, sheath breakdown occurs at high plasma densities [3], and thus there is a limited range of conditions for which this technique is viable [4].

5.2. System Design

The design of our pulsed arc source is based on that of Siemroth *et al.* [5] for a high current pulsed vacuum arc (HCA). Cathodes are 50mm diameter disks with a small hole in the centre for the trigger electrode. A tube of copper is co-axially located in front of the cathode to act as an anode. The trigger is a tungsten wire inserted into an insulating sleeve made of alumina, coaxially inserted through the centre of the cathode. A high-voltage, high power pulse applied between the trigger wire and the cathode causes a flash over to occur across the insulator, igniting an arc that burns between the anode and cathode. Metal plasma is created from the ablated cathode material and expands outward from the cathode surface with a high velocity. A 90° curved solenoid made from copper tubing is located at the exit of the anode and electrically connected in series with the cathode and anode to act as a magnetic macroparticle filter. Cathode, anode and filter can be water cooled to allow a high pulse repetition rate. A schematic of the anode, cathode and trigger, with accompanying photographs, is shown in figure 5.1.

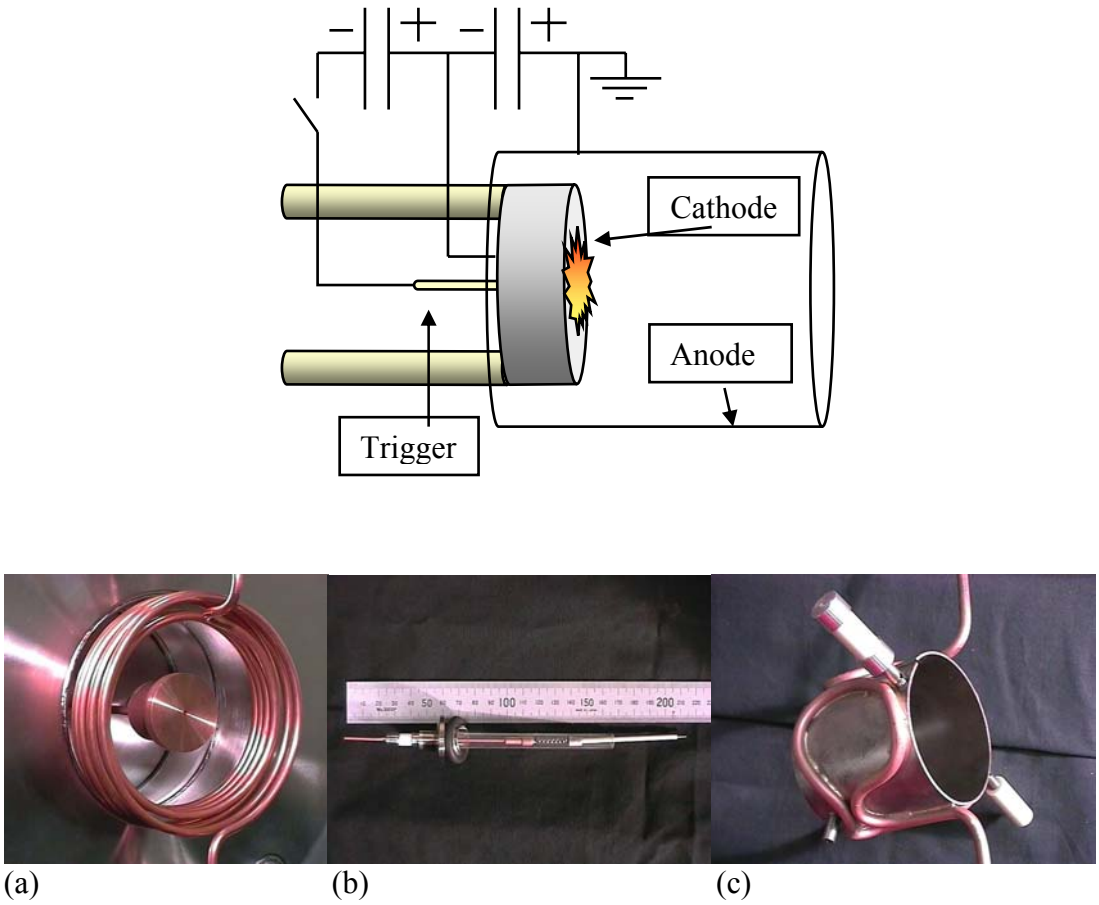

Figure 5.1: Schematic and photographs of the pulsed cathodic vacuum arc described in this chapter. (a): cathode (centre) with magnetic confinement coils. (b): trigger. From left to right; high voltage vacuum feed-through (0-120mm), glass insulating shroud (70-165mm), alumina insulating sleeve (145-205mm), trigger pin (205-215mm). (c): Anode showing water-cooling pipes and insulating holders.

5.2.1 Arc Triggering

Triggering of cathodic arcs is achieved in many ways. Mechanical contact of a biased electrode, laser ablation, high-voltage flashover and the so-called "triggerless" triggering technique [6] are all used to provide the initial plasma to ignite an arc between the anode and cathode (essentially, close the circuit). For a pulsed system the mechanical method is not viable when high repetition frequencies are required. Laser ablation requires an

expensive high power laser. The inventors of the "triggerless" system suggest that the slow rising current profile in high current arcs is not well suited to "triggerless" triggering [7]. Considering these limitations we decided the high-voltage flashover technique was best suited to our requirements.

The high-voltage flashover technique utilizes a high power pulse to ablate a thin conductive film connecting the cathode electrode and a trigger electrode. A common method of arranging these electrodes is to co-axially insert one electrode inside the other and separate them by an alumina insulator. Insertion of the cathode electrode inside the trigger was found by Brown *et al*. to improve the triggering reliability when compared to a centrally located trigger electrode [8]. Whilst this may be the case, we have observed in edge-triggered systems the erosion profile to be concentrated at the edge of the cathode. As will be shown below, this is due to repulsive forces between multiple arc spots. For flat disk cathodes, such as ours, this results in an inefficient utilisation of cathode material and a varying angle of emission of plasma resulting in a variable deposition rate at the substrate. Experiments carried out in our laboratory show that centrally locating the trigger electrode gives a more uniform erosion profile [9]. In addition, optimisation of the arc current can further improve the erosion profile, as discussed below.

Application of a voltage of around 3kV for 3μs between the trigger electrode and the cathode is generally sufficient to create the initial plasma required for triggering of the arc discharge. For successful triggering, the alumina insulator needs to be coated with a small amount of conductive material. Graphite is a good choice. This material is ablated

by the trigger pulse and initiates the conducting pathway to start the arc. After a small number of arc pulses, the alumina becomes partially coated with cathode material from the arc, replacing the ablated graphite.

There is a threshold voltage between the anode and cathode, which must be exceeded to achieve reliable triggering of the arc. For our arrangement this voltage is greater than 100V, however this depends strongly on the arrangement of the anode and cathode. (Note that this is the "pre-burn voltage" and should not be confused with the arc operating voltage, which is generally around 50V). Under these conditions the triggering reliability exceeds 99.9% for around ten thousand pulses. After such a period, the reliability begins to reduce due to a build-up of cathode material on the alumina trigger insulator. By applying of a large power burst (>250 J) to the trigger pin, a large proportion of this build-up can be ablated from the insulator. In this way we have been able to extend the period of reliable triggering by around one thousand pulses.

5.2.2. Anode design

Because the arc is maintained primarily by electron flow between the cathode and anode the electron collecting ability of the anode is an important consideration of the arc design. Many variations on the size and shape of the anode exist in the literature, ranging from tubes and rings surrounding the cathode, to rods axially inserted in the centre of the cathode. [10] For simplicity and historical continuity with our DC design, we chose a tube of copper slightly larger than the cathode diameter and co-axially located around the

cathode. In order to allow operation with a single power supply, the macroparticle filter is connected in series between the anode and power supply. Current collected by the anode is then passed through the filter solenoid to produce the required magnetic field. It is therefore important to insure maximum anode collection efficiency during operation.

With a macroparticle filter installed we compared the anode efficiency for a number of anode lengths. It was found that the distance the anode extended in front of the cathode surface was crucial in determining the anode effectiveness. Figure 5.2 shows a comparison of the current collected in the anode when the anode extended 55 and 70 mm in front of the cathode surface. The 70mm anode closely follows the profile of the cathode current indicating constant collection efficiency. In contrast the 55mm anode exhibits a pronounced droop in current the middle of the arc pulse. A relatively small change in the anode length therefore results in a large difference in the current collected.

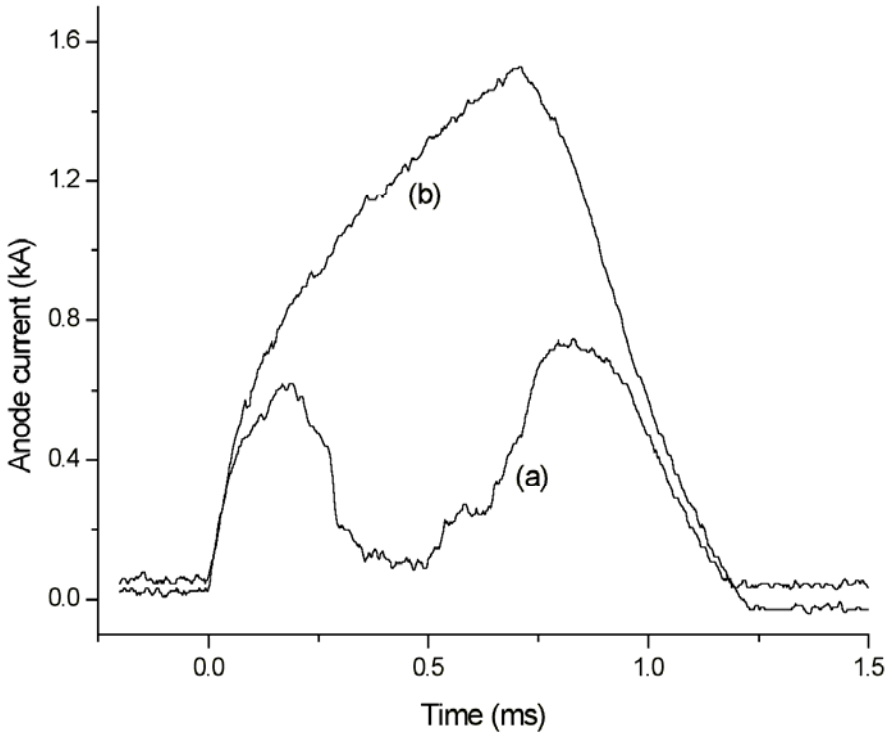

Figure 5.2: Comparison of anode currents collected by; (a) a 55mm long anode; (b) a 70mm long anode.

The angular distribution of plasma flow has been reported to approximately follow a cosine distribution, with higher currents increasing the percentage of ion emission perpendicular to the cathode surface [11]. Increasing the anode length therefore increases the electron current it collects. The magnetic field produced by the filter acts to constrict the flow of the plasma parallel to the cathode surface. Since the current collected by the anode determines the magnetic field strength, there is a feedback mechanism that restricts the current collecting ability for shorter anodes and higher currents. The design of the anode is therefore influenced by the incorporation and design of the magnetic filter. Alternatively the filter can be operated from a separate power supply, reducing the

constraints on anode collection efficiency, but increasing the cost and complexity of the system.

5.2.3. Power supply

For commercially applicable thin film deposition purposes, a pulsed arc must have a deposition rate comparable to other sources. There are two obvious ways to increase the deposition rate: increase the pulse frequency, or increase the arc current. Both these measures are limited by power supply electronics.

In the early stages of prototyping, our power supply consisted of a simple capacitor bank of between 6 and 12 mF, charged to between 100 and 400V. This provided current pulses with a fast rise time and a long decaying tail, such as shown in figure 5.3(a). Since the erosion rate is proportional to the arc current, a current profile such as this results in an excessively high erosion rate near the centre of the cathode where the arc spots are triggered, and a very small erosion rate near the circumference of the cathode. In an attempt to even out the erosion profile across the cathode surface we designed a second power supply with a current profile that increased steadily over the entire pulse (figure 5.3(b)).

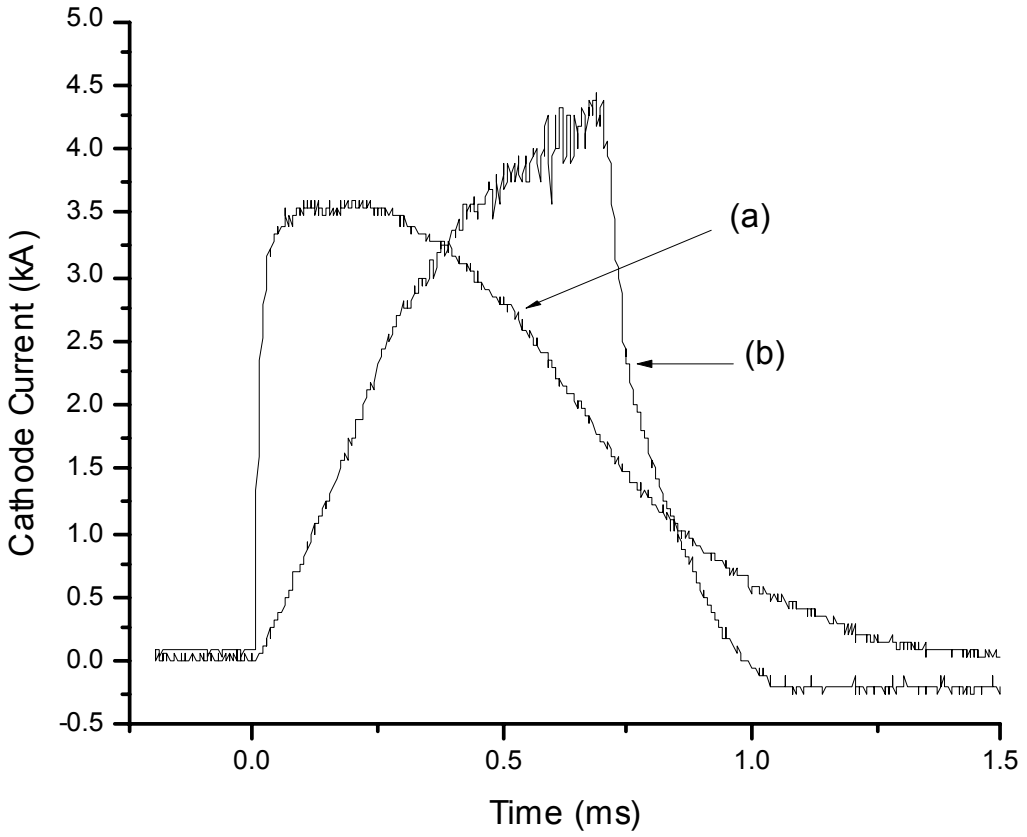

Figure 5.3: Comparison of current profiles for the two power supplies tested; (a) the simple 12mF capacitor bank charged to 400V; (b) the resonant LC circuit, charged to 400V and crowbarred at 0.7ms.

The design was based on an oscillating LC circuit such as that used by Siemroth *et al.* [5], adapted to make it suitable for electrolytic capacitors. Electrolytic capacitors are less expensive for a given capacitance than other types, but require a circuit design that will prevent them from being reverse biased. Both power supplies utilised 1.5mF high-current-discharge electrolytic capacitors manufactured by Lawrence Livermore National Laboratory, California, USA, with a voltage rating of 450V and instantaneous current rating of 417A for 1ms. A circuit diagram of the power supply is shown in figure 5.4. The

oscillation of the circuit follows a sinusoidal profile with a resonance period of a few milliseconds.

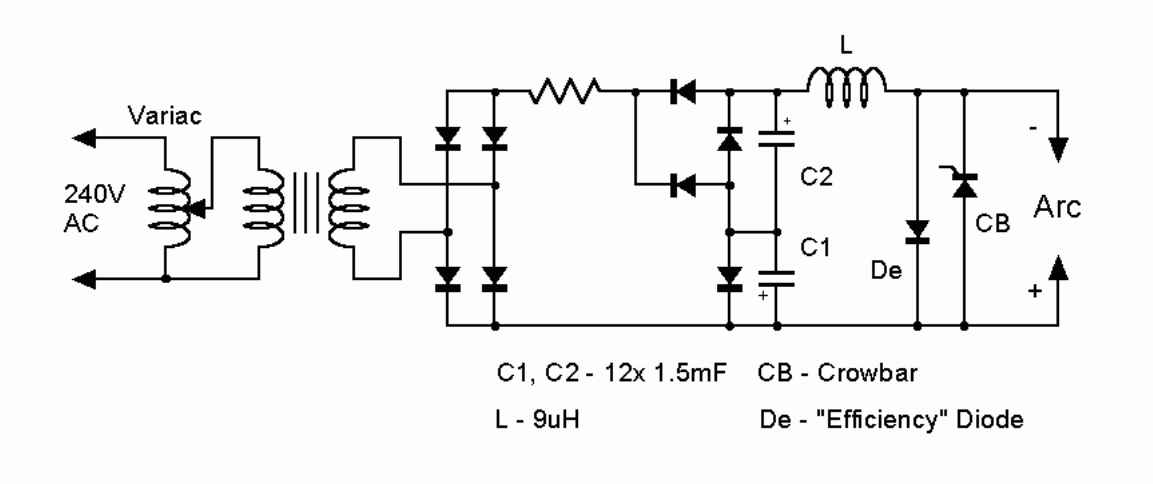

Figure 5.4: Circuit diagram of the resonant LC circuit power supply used to drive the arc current. Diagram by Phil Dennis.

Partway into the cycle the current is interrupted by initiating a "crowbar" action. This effectively short-circuits the capacitor bank, extinguishing the arc current at a specified time. If it is cut prior to the first maximum of the oscillation cycle, a current pulse that rises over almost the entire pulse length is produced. As shall be shown below, different cathode materials exhibit different spot velocities, which in turn determine the time the arc spots take to reach the edge of the cathode. Easy adjustment of the capacitor and inductor values within the power supply is possible, allowing tailoring of the oscillation period for different spot velocities. In figure 5.3(b) the oscillation period is 4ms and the crowbar is initiated after 0.7ms. The ability to change the oscillation period is especially useful for carbon cathodes where the spot velocity is significantly lower than that of most metals, as shown below.

The crowbarring time is adjusted to suit the velocity of the cathode spots so that the maximum coverage of the cathode surface is achieved and the spots do not run over the edge of the cathode surface. The crowbar diverts the current from the plasma but keeps the remaining energy in the circuit. When the current drops to zero the crowbar turns off and the "efficiency" diode takes over, and it carries the entire negative cycle of the current. Efficiency diodes are commonly utilized in high current power supplies (for example [12]). The remaining energy in the circuit is returned to the primary capacitor bank (C1) via the efficiency diode.

We have generally limited the peak ion current to no more than 5 kA to ensure that the system does not overheat. However, during testing, we have run the supply with peak currents as high as 10 kA. Deciding on an optimal peak current requires balancing a number of factors. Since the arc current also provides the current for the coils of the curved magnetic filter, it needs to be high enough to ensure good magnetic confinement (i.e. to produce a field of at least a few tens of milli-Tesla), but it cannot be so high that the force on, and/or heat dissipation in, the filter coils causes them to deform. High arc currents are advantageous because they generate faster moving arc spots due to retrograde repulsion, which produce fewer macroparticles [5]. However, losses in the power supply scale as the square of the peak current. With these factors in mind we designed the power supply to operate with peak currents in the range of 1 to 5 kA.

If the energy of the arriving ions is to be well controlled by the application of a bias voltage to the substrate, it is important that the plasma not only be fully ionised, but that the ion charge state distribution (CSD) is well known. Ions with different charges will

experience unequal acceleration by the application of a bias to the substrate and subsequently exhibit different kinetic energies upon arrival at the substrate. Oks *et al.* [13] showed that the CSD is affected by both the application of a strong axial magnetic field at the cathode surface, and also by the magnitude of the arc current. For a carbon cathode in the absence of an external magnetic field, currents above 2kA linearly increase the average charge state. Thus, although high current arcs can provide a high deposition rate and reduced macroparticle content, it is important to consider the effects of the current on the CSD if the ion arrival energy is to be manipulated by an electric bias. This is also true for the application of an axial magnetic field for the purposes of macroparticle filtering and/or cathode spot motion control. The influence of the magnetic field strength on the ion CSD first becomes apparent for field strengths greater than 0.1T [14].

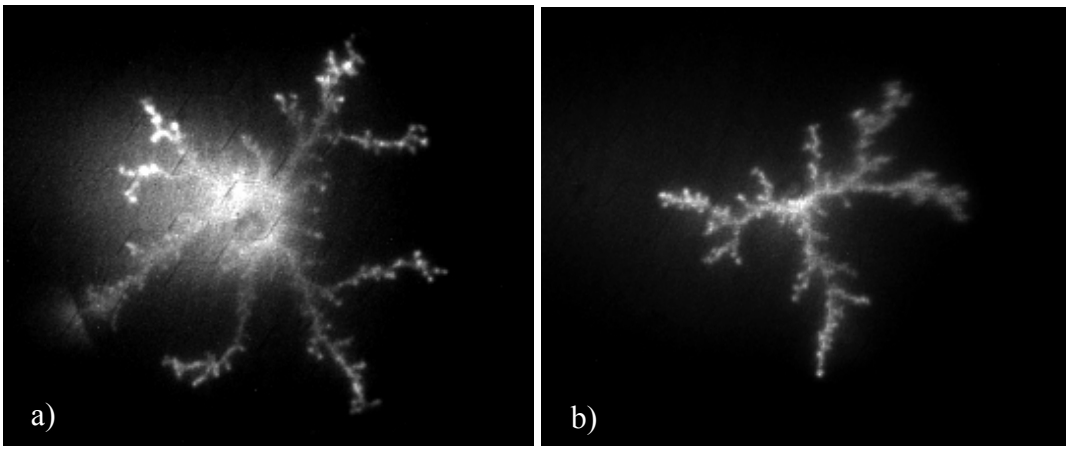

Figure 5.5: CCD camera images of an aluminium cathode. Image (a) shows the high density of arc tracks near the central trigger for the simple 12mF capacitor bank. Image (b) shows the arcing for the oscillating LC circuit, crowbarred after one millisecond. The arcing around the central point of ignition is reduced compared with image (a). Image sizes are 5cm x 5cm.

Compared with the original power supply, the reduction in arc current at the beginning of the pulse reduced the erosion in the centre of the cathode, providing a more even erosion profile over the cathode surface and better utilization of the cathode material. Figure 5.5

consists of two CCD camera images of arc traces for the two different power supplies, showing the reduction in the arcing, and hence the erosion, near the centre trigger for the oscillating LC power supply.

Figure 5.6 illustrates the spatial distribution of arcing in a different way. A series of 1μs exposures of the light emission from the arc spots were taken at different times into the arc pulse for the two different power supplies. The time period covered by the frames corresponds to the first 600μs of the current profiles shown in figure 5.3(b). The fast rising current of the 12mF capacitor supply, shown in series A, produces many spots at the beginning of the pulse which quickly repel one another toward the edge of the cathode. The spot velocity is reduced at the end of the pulse since the current is beginning to fall and the inter-spot distance is large. In contrast, the slow rising current of the optimised power supply, shown in series B, starts out with only a few spots, which radiate outward at a much lower (but ultimately more even) velocity due to the weaker repulsive forces. The spot velocities in both images are proportional to the number of spots (i.e. the current) and the distance the spots have travelled, since the repulsive forces increase with current and decrease with the distance between the spots. Further optimisation of the current profile for efficient utilisation of the cathode material requires careful consideration of these competing effects.

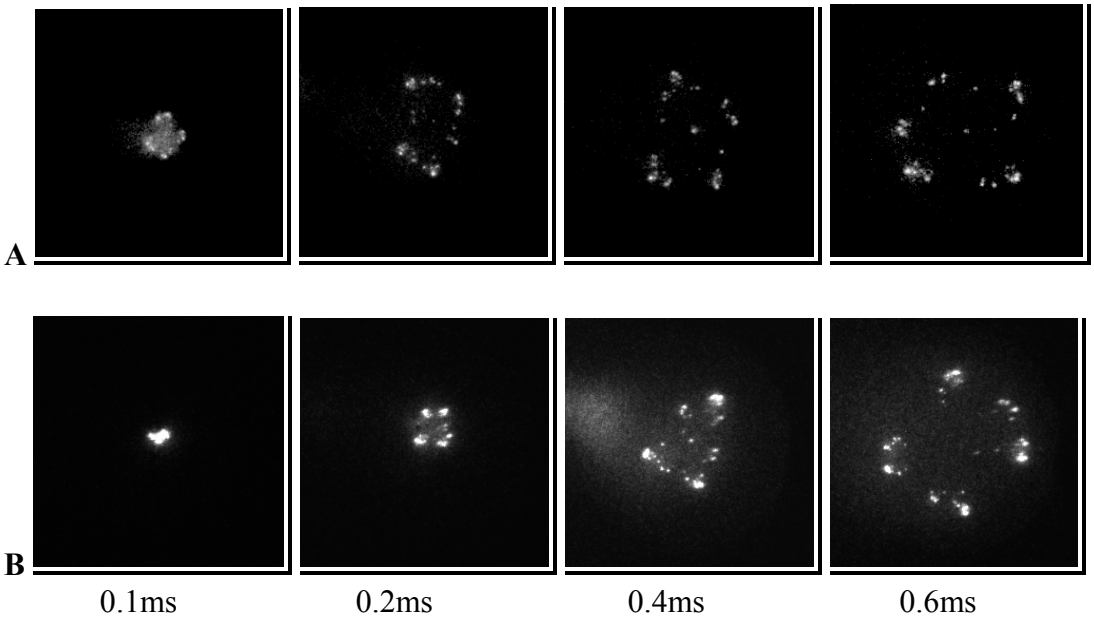

Figure 5.6: CCD images of arc spots on an aluminium cathode taken during an arc pulse. All exposures are 1μs in duration taken 0.1, 0.2, 0.4 and 0.6 ms after ignition, from left to right respectively. The upper series (A) shows the spot locations for the 12mF power supply and the lower series (B) for the oscillating LC circuit.

The crowbar restricts the arc spots from running over the edge of the cathode and, either arcing on material that would contaminate the plasma, or forming a breakdown to the anode or chamber walls. A particularly good example of why breakdown to the anode should be avoided is presented in figure 5.7. In this image, the arc has run over the edge of the cathode, probably due to fast moving type-1 spots encouraged by cathode contamination (discussed below). A runaway arc discharge has been established between the anode and cathode before the crowbar was initiated, channelling the entire energy of the capacitor bank. An anode spot is formed on the anode that ablates the anode material, contaminating the plasma and damaging the electrode. This demonstrates the need for proper conditioning of the cathode to remove surface contamination. Monitoring the time taken for the arc spots to reach the edge, and initiating the crowbar at the appropriate

time, allows the erosion to be controlled to utilize as much of the cathode as possible without allowing the arc to run over the edge.

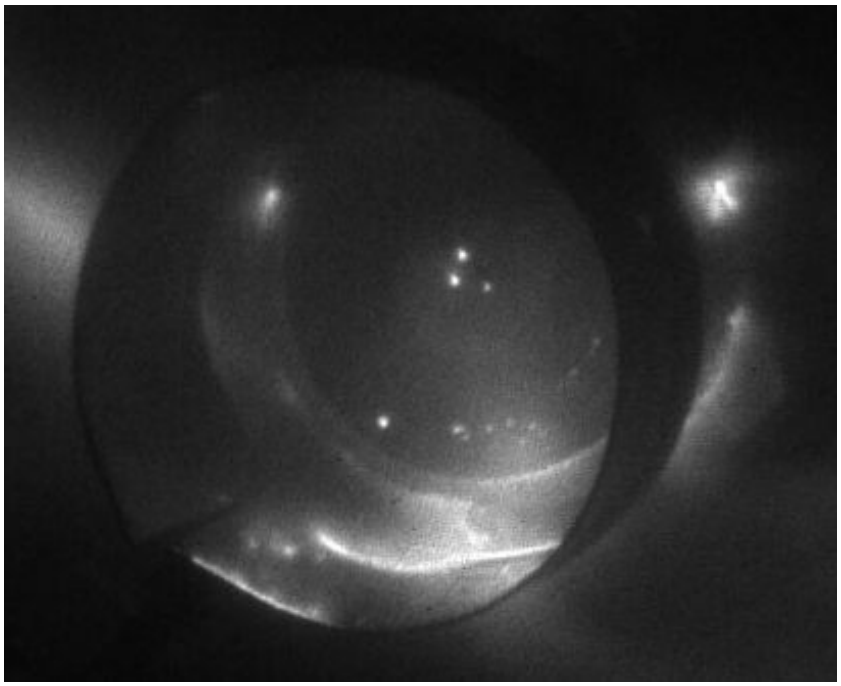

Figure 5.7. Arcing between cathode (centre circle) and anode (outer tube) caused by the cathode spots running over the edge of the cathode and forming an arc discharge to the anode (bottom).

5.3. Cathode spots in a high current pulsed arc

5.3.1 Retrograde motion and spot velocities

As discussed in chapter 3, high-current arcs exhibit simultaneous multiple arc spots on the cathode surface. The resultant magnetic field drives each spot is in the retrograde direction [15]. Whilst extensively documented, the origins of these retrograde directional forces are poorly understood. The retrograde directional force appears as a repulsive

force between the spots and, as such, high-current arc spots move outward from the ignition point. This is observed in images of high current arc traces showing dendritic patterns radiating outward from the point of ignition (figure 5.8). As discussed in chapter 3, each spot has a lifetime characteristic of the cathode material and surface conditions. Generation and extinction of spots, followed by generation of one or more spots at new locations on the retrograde side, is responsible for the dendritic nature of the arc motion.

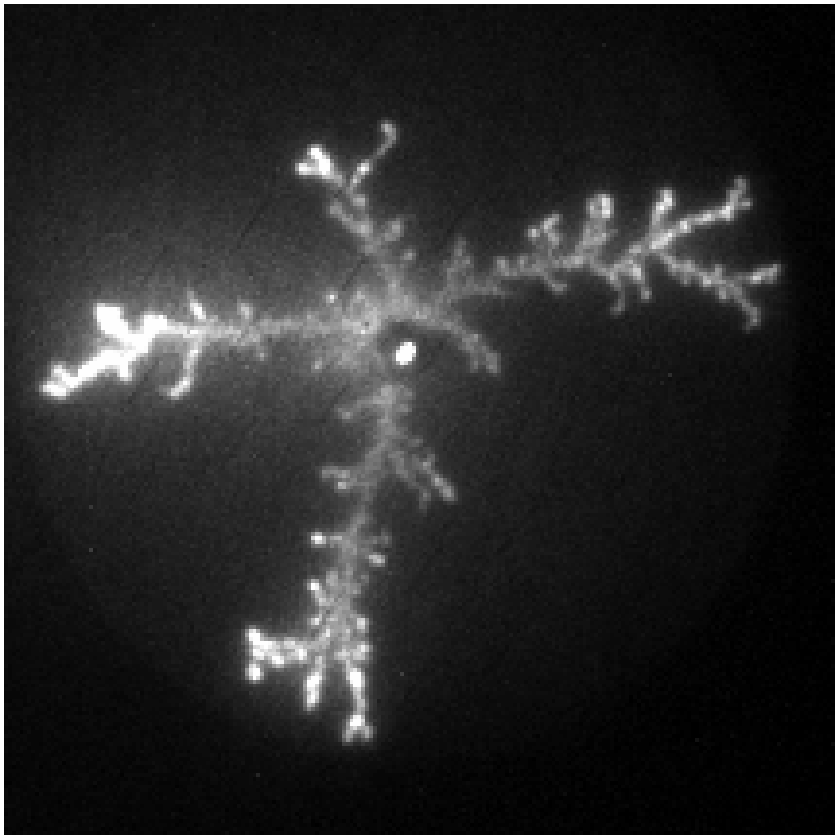

Figure 5.8: CCD image of a typical arc trace on an aluminium cathode. The arc spots radiate outward from the point of ignition due to retrograde forces. Image size 5cm x 5cm.

Spot velocities are dependent on the cathode material, the total current carried by the arc and the distance from the ignition point. To investigate the velocity of the cathode spots a series of short exposure CCD camera images were taken of arcs on titanium, aluminium

and carbon cathodes by a Princeton Instruments ICCD camera with a ST-138 control unit. 1μs exposures were taken at various times after triggering. An arc bank voltage of 200V was used in all cases, corresponding to a peak arc current of 2.2kA, with a profile the same as that shown in figure 5.3(b).

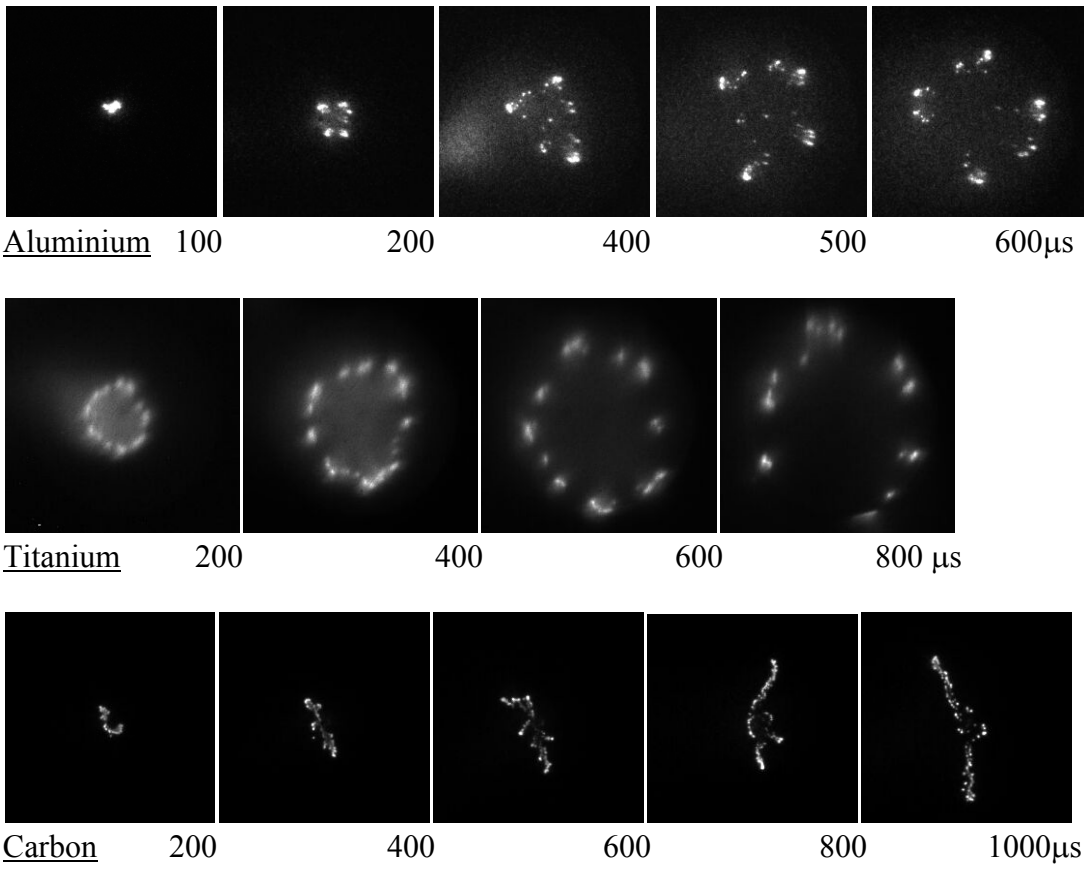

Figure 5.9: 1μs exposures of arcs on aluminium, carbon and titanium cathodes. The numbers shown are the time elapsed since triggering. Image sizes Al & C: 52 x 52mm. Ti: 58 x 58mm. All images are to scale 1:1.9.

The cathode spot images are shown in figure 5.9. Of note is the difference in sub-group structure between the different cathodes. Titanium arc spots are quite distinct and of fairly equal intensity, radiating outward in an even circle. Aluminium spots aggregate into 4 or 5 groups containing 5 or more spots. Carbon spots appear long-lived and remain

confined to within a few branches. An active bright spot appears at the end of each branch in the carbon images, inner spots slowly fading in intensity.

An estimate of the number of spots in each of the 600μs images was made. This effort was complicated by the poor resolution of the images. Some spots appear to be elongated suggesting a number of unresolved spots. Only the brightest spots were counted in the carbon images. The estimates are shown in table 5.1. Also tabled is the current per spot, determined by dividing the number of spots by the arc current at 600μs (1.9kA). These values are compared with values for the current per spot from reference [16]. The currents per spot determined by this simple analysis are significantly higher than those from the literature. In all cases the measured value is around 1.4 times the published value. This would suggest that many of the individual spots are not clearly resolved in the images above. A statistical analysis of many higher resolution images is necessary to conclusively determine these values.

Table 5.1: Number of cathode spots and current per spot for three different cathode materials at 600μs. The current at this point was 1.9kA.

Cathode	**# Spots**	**Amperes/spot**	**Amps/spot ref** [16]
Al	33	58	30-50
Ti	19	100	70
C	7	270	200

The images shown in figure 5.9 are to scale with one another. Comparison of the 600μs images in all three series shows that the titanium spots move with the highest velocity, followed by aluminium and carbon. These results do not follow the same trend as the numbers of arc spots. We may expect larger numbers of spots to exert increased

retrograde repulsion on one another. This assumption is incomplete since we need to account for the total current in all the spots and the inter-spot distances as well. The approximate radius of the circular arrays of arc spots was measured and the results are shown in figure 5.10. For the carbon arcs an estimate of the distance of the spot farthest from the trigger point was made.

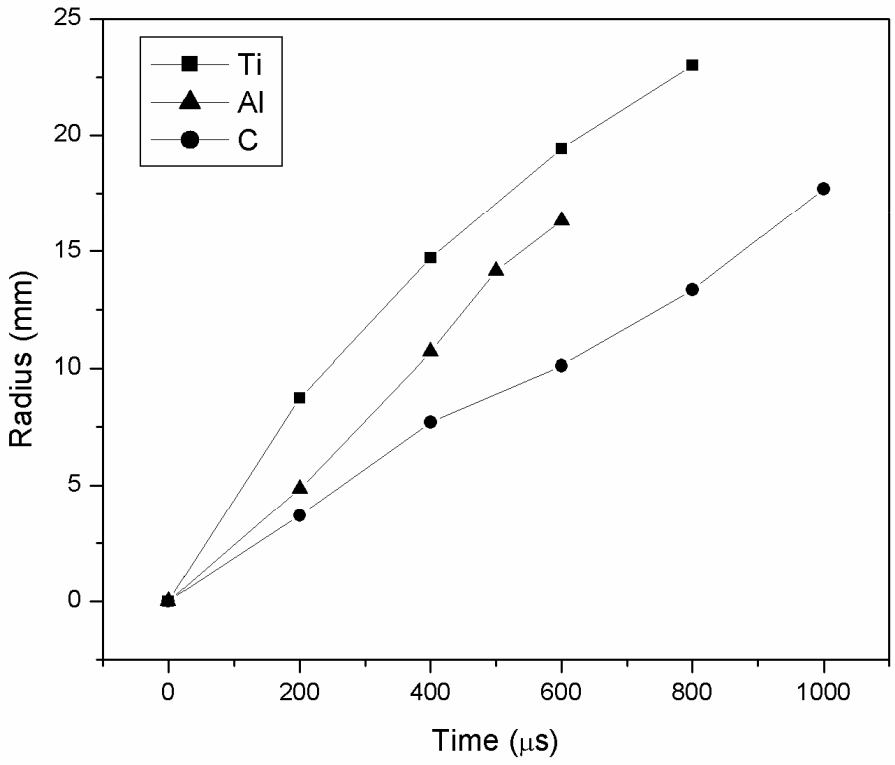

Figure 5.10: Arc spot radii as a function of time for different cathodes from the images in figure 5.9.

To accurately model the spot velocities in terms of the retrograde forces it would be necessary to include the effects of the current profile and the inter-spot distances. The current profile is known to vary as the first quadrant of a sinusoid over 1ms. As mentioned in chapter 3, the physical mechanisms responsible for retrograde motion are

not well understood. If we conjecture a magnetic repulsion opposite but equal to the attractive force, per unit length, exerted by two current carrying wires on one another, we expect a dependence proportional to the inverse of the distance between the spots. In the case of titanium, where there are many spots on the circumference of a circle, it may be possible to model the spots as a complete ring of current, integrating the force in radial co-ordinates. In the case of aluminium, the spots are not radially symmetric and the situation is even worse in the case of carbon. Modelling the velocities of the arc spots in high current arcs is therefore a complicated process and is not attempted here.

A reduction in macroparticle emission has been observed for high current arcs [5] and arcs operating in high magnetic fields [17]. The increased current results in an increase in spot velocity. This reduces the dwell time of the cathode spots in any given area, thus reducing the local heating and reducing the amount of molten cathode material that can be incorporated in the plasma.

5.3.2 Spot types

When a new cathode was installed into the system it was observed that the arc operated in a different mode to that when the same cathode had been employed for some time without breaking vacuum. Review of the literature revealed this to be due to the existence of two types of arc spots, historically labelled type-1 and type-2 arc spots [18]. Type-1 is the term used for arc spots with comparatively high velocity, low brightness and low arc current per spot. Conversely type-2 spots exhibit comparatively low velocity, high

brightness and high current per spot [15, 19, 20]. Type-1 arc spots are attributed to the burning of surface contaminants and adsorbed gases on the cathode surface. Due to their higher velocity and low currents, very little ablation of the cathode material occurs and they are therefore undesirable for the production of metal plasmas.

In their original paper on the HCA, Siemroth *et al.* [5] present high-speed photographs of arc spots moving radially outward from the point of ignition. Comparing the time period between ignition and when the spots reach the edge of the cathode with other images of arc traces in the same work shows that the arc spots in these high-speed images move at a much faster velocity. We conjecture that type-1 spots are observed in the high-speed photographs and type-2 spots are observed in subsequent images. However, no such distinction was made by the authors, indicating that they may not have identified the two types of spot mode.

Our experiments showed that operating the arc for around 100 pulses is sufficient to "condition" the cathode: that is, remove all surface contaminants by ablating them in the type-1 mode. Subsequent arc pulses operate in a type-2 mode, exhibiting lower spot velocities and higher currents, ablating the cathode material itself to form a pure metal plasmas. Figure 5.11 shows a series of 3 CCD images taken after a new cathode was inserted into the system using the original simple power supply. For the first 40-odd pulses the arc operated in a type-1 mode (figure 5.11(a)), with the spot traces reaching the edge of the 51mm diameter cathode in less than 200μs. After 49 pulses the arc is observed to be operating initially in a comparatively bright type-2 mode before reverting

back to a type-1 mode of operation as the arcs spots encounter contaminated regions of the cathode towards the edges.

Arc spots preferentially occur where there is a reduction in the work function of the surface due to increased electron emission in that region [21]. Since adsorbed gases on the cathode surface reduce the work function [21] the arc will preferentially burn in a type 1 mode on contaminated regions of the cathode. This shows that the inner regions of the cathode have been cleaned by arcing, whilst the outer regions are still contaminated. After 62 pulses the arc is operating entirely in a type-2 mode, exhibiting comparatively slow moving arc spots, which are still within the cathode boundary after 1ms. The slow transition (~20 pulses) from completely type 1 to completely type 2 arc modes further illustrates the uneven arcing distribution when using the simple power supply.

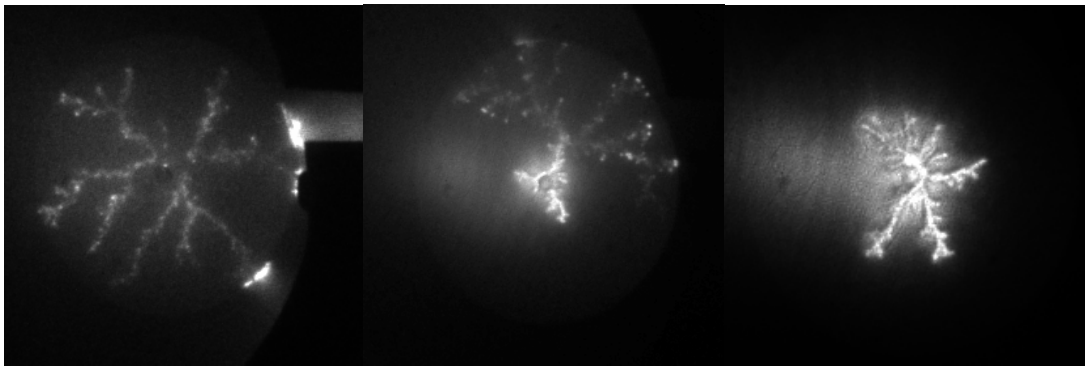

(a) (b) (c)

Figure 5.11: CCD images of an aluminium cathode showing the transition from type I spot mode to type II mode. Image (a) is taken 8 pulses after the cathode was inserted into the vacuum system (exposure time 0.2ms). After 49 pulses (b) the arc begins to operate initially in a type II mode before reverting to type I as contaminated regions are reached (exposure time 0.3ms). After 62 pulses (c) the cathode surface has been cleaned of contaminants and the arc is operating purely in type II mode (exposure time 1ms). Image sizes are 6cm x 6cm.

When the optimised power supply was used, the conditioning of the cathode was improved by cleaning the entire surface of the cathode, including the outer regions, at roughly the same rate. As a result the transition from type-1 to type-2 spot modes was more abrupt, occurring within a few arc pulses. A Pfeiffer "Prisma" mass spectrometer residual gas analyser was attached to the vacuum chamber during the operation of the pulsed arc source. Residual gas measurements, shown in figure 5.12, show a sharp change in the gas species present. This corresponds exactly to the observed transition from type-1 to type-2 behaviour. From the trace we can see that hydrocarbon fragments and CO_2 are higher during the type-1 phase than during the type-2 phase, while oxygen and nitrogen are highest in the type-2 phase. This is consistent with the understanding that spots in the type-1 mode preferentially burn a contamination layer (often of hydrocarbon) off the cathode surface, while type-2 spots are those ablating a clean cathode surface.

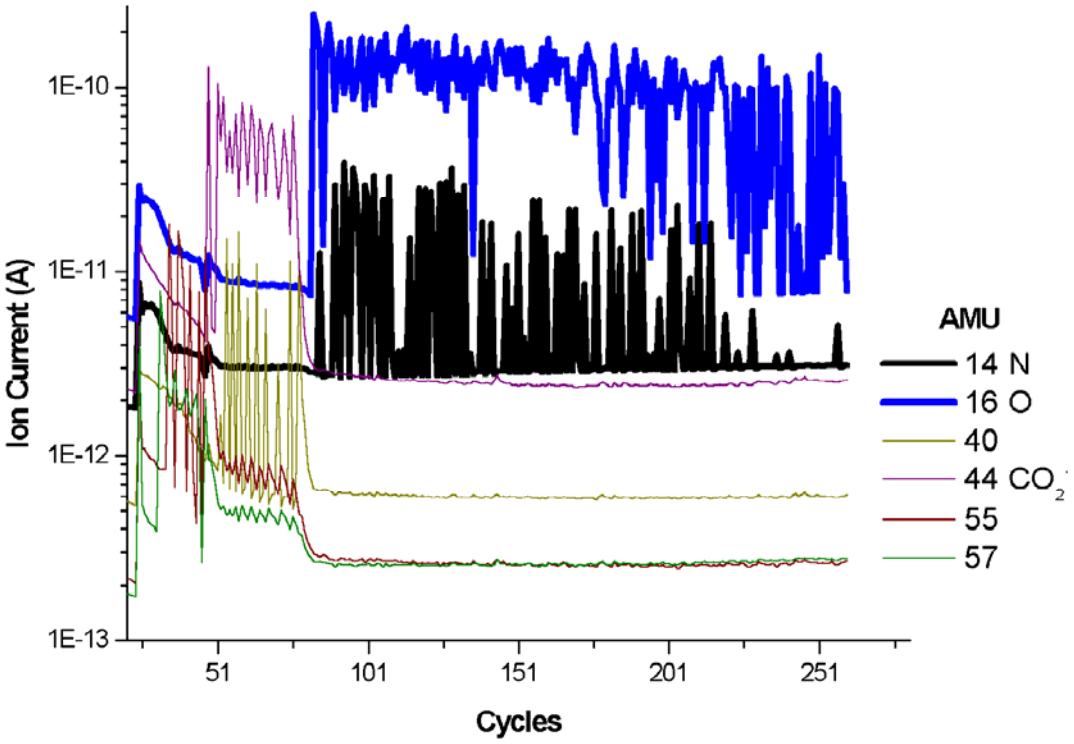

Figure 5.12: Mass-spectrometer gas analysis. The heavy lines are AMU 16 and 14 from top to bottom (most probably oxygen and nitrogen respectively). The light lines from top to bottom are AMU 44, 40, 55 and 57. AMU 44 could be CO_2 while the others are most likely to be hydrocarbon fragments.

It has been reported recently that the composition of a pulsed vacuum arc plasma operated in an oxygen environment shows a dependence on the arc pulse frequency [22]. This is due to the formation of monolayers of gas on the surface of the cathode. It is recommended that the arc be operated at a frequency high enough to avoid the adsorption of significant amounts of gaseous contaminants to the cathode surface. This minimum frequency will depend strongly on the background gas pressure. At gas pressures of $1x10^{-6}$ torr, the formation rate of a monolayer of gas on a surface at room temperature is of the order of one second. Therefore the arc pulse frequency of 0.5 Hz used to obtain the

data in figure 5.12 is insufficient to prevent the formation of adsorbed gas layers on the cathode surface between pulses. It is not surprising then to observe the presence of nitrogen and oxygen in the mass spectrometer trace when the arc is operating in a type-2 mode under these conditions.

The presence of nitrogen and oxygen in the gas analysis during the type-2 phase may also be due to the arc ablating oxide and nitride compounds from the cathode surface. Both species are observed to decrease with time, with nitrogen falling off to levels observed before the type-2 phase, which is consistent with the removal of these compounds. The reduction may also be explained by heating of the cathode surface reducing the amount of gas condensation between pulses.

5.4 Operational performance

We have successfully operated the arc with a number of cathode materials, including carbon, aluminium, titanium, silver and copper. For initial characterisation of deposition rates, titanium films were deposited on silicon substrates, both in front of and after the macroparticle filter. Deposition rates were measured by determining the final film thickness using a stylus profilometer. At a location 100mm from the cathode surface, without the macroparticle filter employed, the deposition rate was determined to be 1.7 ($^{+}$/- 0.1) nm per arc pulse. For these measurements the oscillating LC power supply was used at a peak arc current of 3kA (arc bank 210V). For short operating periods we have successfully operated the system at frequencies as high as 50 Hz. This corresponds to a

time averaged deposition rate of 85nm.s^{-1} for titanium. This rate is not large in comparison with a carbon deposition rate of 200nm.s^{-1} from Siemroth's HCA [23], measured 150mm from the source at a pulse frequency of 300Hz. At this stage we have not thoroughly investigated the fundamental limits of the pulse frequency for our system. Limits on pulse frequency are set primarily by the heat tolerance of the circuit components.

Deposition rates after the macroparticle filter were significantly lower, at around 0.07nm per arc pulse. At only 4% of the deposition rate before the filter entrance this represents a significant loss of the plasma available for deposition. Research is ongoing into the optimisation of the filter transport efficiency. With the macroparticle filter employed we have used a Langmuir probe to measure ion densities greater than 1x10^{19} m^{-3} at the substrate position for a titanium plasma. At 50Hz the time averaged ion density is around 3 x 10^{17} m^{-3}, which is an order of magnitude greater than the ion densities measured in our DC arcs (section 3.4.2.1.). With significant deposition rates demonstrated in the unfiltered arrangement, macroparticle filter efficiency is the primary limiting factor of the deposition rate. Optimised filter arrangements have indicated filter efficiencies as high as 35% (defined as ratio of plasma density at entry and exit of filter) for an in-plane 90° magnetic filter [24]. If filter efficiency can be improved to this level in our system then time averaged metal ion densities in excess of 1 x 10^{18}cm^{-3} can be achieved.

5.5 Conclusion

We have designed and tested a pulsed cathodic arc source capable of generating high density metallic plasmas with highly reproducible plasma characteristics. There are two ways to increase the deposition rate of a pulsed arc: increase the current or increase the frequency. The primary drive in the work presented here has been to explore the increased current option. In hindsight I would suggest that further research be done on increasing the frequency with the aim of finding a middle ground between frequency and current. Central triggering combined with a tailored current profile was shown to be an effective method of controlling the erosion profile of the cathode surface. The arc current should be maintained at a level high enough to retain the advantages of the retrograde repulsion due to multiple arc spots; namely, reduction in macroparticle emission and enhanced control of the erosion profile.

A reduction in instantaneous plasma density would not be of great concern if the time-averaged density can be maintained. Since the heating of the components scales with the square of the current, this would also lessen concerns of overheating. A reduced peak current would also reduce safety concerns. Ion charge states could be confidently predicted from literature, and filtering of the large plasma currents would be simplified. For plating free implantation by the application of a DC bias to the substrate, a smaller capacitance would be required and there would be less chance of breakdown at lower plasma densities. Breakdown often occurs after a certain period of implantation due to enhanced fields at the surface caused by ion impact heating resulting in out-gassing. This

is especially prominent during implantation of polymers. A shortened pulse length may circumvent this limitation. Therefore a shorter arc pulse and reduced cathode diameter may also be advantageous.

5.6 References

1. Sroda, T., S. Meassick, and C. Chan, Applied Physics Letters,, 1992. **60**(9): p. 1076.
2. Brown, I.G., Monteiro, O.R., Bilek, M.M.M., *High voltage sheath behaviour in a drifting plasma.* Journal of Applied Physics, 1999. **74**(17): p. 2426-2428.
3. Anders, A., *Width, structure and stability of sheaths in metal plasma immersion ion implantation and deposition: measurements and analytical considerations.* Surface & Coatings Technology, 2001. **136**(1-3): p. 85-92.
4. Bilek, M.M.M., *Effect of sheath evolution on metal ion implantation in a vacuum arc plasma source.* Journal of Applied Physics, 2001. **89**(2): p. 923-927.
5. Siemroth, P., T. Schulke, and T. Witke, *High-Current Arc - a New Source for High-Rate Deposition.* Surface & Coatings Technology, 1994. **68**: p. 314-319.
6. Anders, A., et al., *Triggerless Triggering of Vacuum Arcs.* Journal of Physics D-Applied Physics, 1998. **31**(5): p. 584-587.
7. Anders, A., R. Macgill, and T. McVeigh, Review of Scientific Instruments, 1999. **70**(12): p. 4532.
8. Brown, I.G., *Vacuum arc ion sources.* Review of Scientific Instruments, 1994. **65**(10): p. 3061-3081.

9. Gan, B.K., et al., *Optimizing the triggering mode for stable operation of a pulsed cathodic arc deposition system.* Plasma Sources Sci. Technol., 2003. **12**: p. 508-512.

10. Berthold, J., T. Witke, and P. Siemroth, *Vacuum arc evaporator*. 2000: USA patent no. 6,361,663.

11. Fuchs, H., H. Mecke, and M. Ellrodt, *Distribution of ion current density in a modified pulse arc process as a function of pulse parameters.* Surface & Coatings Technology, 1998. **98**: p. 839-844.

12. MacGill, R., I.G. Brown, and J.E. Galvin, Review of Scientific Instruments, 1990. **61**(1): p. 580.

13. Oks, E.M., et al., *Ion Charge State Distributions in High Current Vacuum Arc Plasmas in a Magnetic Field.* IEEE Transactions on Plasma Science, 1996. **24**(3): p. 1174-1183.

14. Oks, E.M., *Generation of multiply-charged metal ions in vacuum arc plasmas.* IEEE Transactions on Plasma Science, 2002. **30**(1): p. 202-207.

15. Juttner, B., *Cathode spots of electric arcs.* Journal of Physics D: Applied Physics, 2001. **34**: p. R103-R123.

16. Lafferty, J.M., *Vacuum arcs. Theory and applications.* 1980, New York: John Wiley & Sons.

17. Swift, P.D., *Experimental investigations of the cathodic arc*, in *PhD Thesis*. 1991, University of Sydney: School of Physics.

18. Harris, L.P., in *Vacuum arcs: Theory and Application*, J.M. Lafferty, Editor. 1980, John Wiley and Sons: New York.

19. Anders, S. and A. Anders, *On modes of arc cathode operation.* IEEE Transactions on Plasma Science, 1991. **19**(1): p. 20-24.

20. Anders, S. and B. Juttner, *Influence of Residual Gases on Cathode Spot Behavior.* IEEE Transactions on Plasma Science, 1991. **19**(5): p. 705-712.

21. Anders, S. and B. Juttner, IEEE transactions on plasma science, 1991. **19**(5): p. 705-712.

22. Schneider, J.M., et al., *Temporal development of the plasma composition of a pulsed aluminum plasma stream in the presence of oxygen.* Applied Physics Letters, 1999. **75**(5): p. 612-614.

23. Siemroth, P., et al., *Short-Time Investigation of Laser and Arc-Assisted Deposition Processes.* Surface & Coatings Technology, 1994. **68**: p. 713-718.

24. X.Shi, et al., Thin Solid Films, 1999. **345**: p. 1-6.